

# Communication

## Theoretical Study of Alpha Case Formation during Titanium Casting

R.G. KEANINI, GREGORY K. WATKINS, TORU OKABE, and MARIE KOIKE

Scale analyses indicate that three distinct contaminant mass-transfer processes, occurring on distinct time scales, underlie formation of the alpha case on small titanium castings. High rates of mold-to-liquid metal mass transfer occur during an extremely short induction period, the length of which is determined by the time required for heterogeneously nucleated solidification fronts to cover mold surface asperities. Following the induction period, but prior to complete cast solidification, mold contaminants diffuse through a rapidly growing solidification layer, where the solid-phase mass-diffusion boundary layer grows at a rate approximately an order of magnitude slower than the solidification front. Finally, following complete solidification and until the part is removed from the mold, contaminant mass transfer continues *via* solid diffusion. Based on the scale analyses, an analytical model that incorporates an empirical relation between titanium solid phase oxygen concentration and titanium microhardness is developed and compared against representative experimental near-surface microhardness measurements.

DOI: 10.1007/s11663-007-9058-x

© The Minerals, Metals & Materials Society and ASM International 2007

---

Due to the extreme reactivity of liquid titanium with most constituents and contaminants found in typical cast molds,<sup>[1,2]</sup> titanium castings are subject to formation of a thin, hard, brittle surface layer, commonly referred to as the alpha case. Although the formation of the alpha case is well known and accommodated for within the titanium casting community, a detailed understanding of both the dynamics and transport phenomena associated with its formation remains elusive. The purpose of this article is to first examine, *via* scaling analyses, some of the essential thermophysical features underlying the process, and then, based on the scaling analysis, to develop a simple mathematical model of the process.

---

R.G. KEANINI, Associate Professor, Department of Mechanical Engineering and Engineering Science, and GREGORY K. WATKINS, Assistant Professor, Department of Mechanical Engineering Technology, are with The University of North Carolina at Charlotte, Charlotte, NC 28223-0001. Contact e-mail: rkeanini@uncc.edu TORU OKABE, Regent's Professor and Chair, and MARIE KOIKE, Assistant Professor, are with the Department of Biomaterials Science, Baylor College of Dentistry, Texas A&M University System Health Science Center, Dallas, TX 75246.

Manuscript submitted November 3, 2006.

We focus on the casting of small parts, *i.e.*, those having characteristic dimensions on the order of  $10^{-2}$  m or less, because at these scales, the presence of an alpha case impacts cast part mechanical properties much more severely than at larger scales. In addition, because we will derive a model describing formation of the alpha case and then will compare the model against a particular, though representative set of, experimental measurements,<sup>[3]</sup> we focus on the case of casting within a drop cast hearth using a nonconsumable arc heat source.<sup>[3]</sup> Nevertheless, the basic physical processes and model described here will have application to a wide range of casting operations.

In the experiment cited,<sup>[3]</sup> 20-mm-diameter Ti rods were cast in zircon sand molds, where, as a means of varying mold oxygen content, the molds were pre-fired for 2 hours at four different temperatures, 873 K, 1073 K, 1273 K, and 1473 K, prior to casting. Once cast, the rods were cut and, among various tests, subjected to microhardness measurements and microstructural study.

We first determine, qualitatively, the sequence of events that occurs within the casting, beginning from the instant that a drop of liquid Ti first falls into the mold. Thus, initially, based on a number of measurements of microhardness,  $H$ ,<sup>[3,4]</sup> showing that  $H$  remains essentially invariant beyond a certain subsurface depth, we conclude that a short *induction period* exists prior to the initiation of inward solidification from the mold surface. During this induction period, due to the motion of the molten drop impinging on the mold, solidification is largely suppressed and reactive mold constituents rapidly pass into the liquid Ti.

Focusing initially on solidification in molds, *e.g.*, sand molds, having relatively rough surfaces, we argue that due to near-zero fluid velocities and low mold surface temperatures, heterogeneous solidification is first initiated within the small asperities that permeate such mold surfaces. Indeed, this process represents the solid-liquid phase change analog to heterogeneous boiling (liquid-vapor phase change) that occurs when vapor cavities spontaneously form within (and subsequently grow from) superheated asperities in heated surfaces.<sup>[5]</sup> The induction period time scale,  $\tau_I$ , is thus determined by the time required for solidification nuclei to grow from surface asperities to some characteristic depth,  $\epsilon_a$ . While it is tempting to identify  $\epsilon_a$  as the average surface roughness, bulk microhardness measurements, which show similar values in titanium samples cast in both sand and investment molds<sup>[7]</sup> (where the average roughness of the latter is approximately an order of magnitude smaller than in the former<sup>[8]</sup>), suggest that  $\epsilon_a$  corresponds to an asperity scale smaller than the average roughness of sand molds. Importantly, we recognize that throughout the induction period, reaction products and contaminants from the mold pass *via* diffusion into the liquid Ti. As noted by Saha,<sup>[3]</sup> due to the high diffusivity of most constituents in liquid Ti, and due to turbulent dispersion, these contaminants are spread uniformly throughout the liquid phase.

We envision a typical asperity as a cone- or rod-shaped cavity that has a characteristic depth  $\epsilon_a$  and a similar characteristic diameter (of order  $\epsilon_a$ ). In order to

obtain an estimate of  $\tau_I$ , we first estimate the characteristic time-dependent heat flux,  $q$ , passing through the asperity (from liquid metal to mold) as  $q \approx k_l \Delta T / \delta(t)$ , where  $k_l$  is the characteristic thermal conductivity of the liquid metal,  $\Delta T$  is the characteristic temperature difference between the initial temperatures of the liquid metal and mold,  $T_0$  and  $T_{mo}$ , respectively ( $\Delta T = T_0 - T_{mo}$ ), and  $\delta(t)$  is the time-dependent thermal boundary layer thickness (which grows outward from the asperity surface into the liquid).

Using the standard energy equation,  $\rho C_p DT/Dt = \nabla \cdot k \nabla T$ , where  $DT/Dt$  is the material derivative and where advective transport terms on the left are negligible within any given asperity, we obtain an order of magnitude estimate for  $\delta(t)$  by balancing the surviving time derivative term on the left with the dominant conduction term on the right, yielding  $\delta(t) \approx \sqrt{\alpha t}$ , where  $\alpha$  is the thermal diffusivity. Next, we recognize that, in an order of magnitude sense, the flux passing through the asperity will be on the order of the latent heat release generated as the liquid starts to solidify at the asperity walls, or  $q \approx k_l \Delta T / \sqrt{\alpha t} \approx \rho U_a L$ , where  $\rho$  is the liquid density,  $U_a$  is the characteristic speed of the growing solidification front, and  $L$  is the latent heat of fusion. In addition, we note that the time required for the solidification front to grow out of the asperity, which again we identify as  $\tau_I$ , is on the order of  $\tau_I \approx \epsilon_a / U_a$ . Combining this estimate with the latent heat energy balance immediately above and solving for  $\tau_I$  then yields  $\tau_I \approx \alpha \rho^2 L^2 \epsilon_a^2 / (k_l^2 \Delta T^2)$ . Using characteristic values for each of the parameters in this estimate (Table I), we then obtain  $\tau_I \approx 2(10^4) \epsilon_a^2$ . Although existing data are insufficient to estimate  $\epsilon_a$  and thus  $\tau_I$ , an upper bound on  $\tau_I$  is obtained using the average roughness of sand molds,<sup>[8]</sup> thus, using  $\epsilon_a \approx 2.5(10^{-5})$  m, we find  $\tau_I^{(max)} \approx 1.25(10^{-5})$  seconds.

Once solidification ensues at the mold surface, the solidification front grows into the liquid metal; due to lower solid-phase diffusivities, mass transfer of mold constituents and reaction products into the casting becomes suppressed and a mass transfer diffusion layer begins to form in the solidified metal. Thus, a key question, which bears directly on how solid phase mass transfer should be modeled, arises as to the relative rates of growth of the solidification front and the solid-phase mass-transfer diffusion layer. If the diffusion layer grows much faster than the solidification front, then we would expect to see a nearly uniform distribution of contaminants within the solidified casting. In this limit, the

equation governing solid-phase mass transfer,  $C_{,t} = \nabla \cdot D \nabla C$ , simplifies to a spatially lumped model. On the other hand, if the solidification front grows much faster than the mass-transfer diffusion layer, then we will observe a concentration boundary layer frozen into the solidified casting; mathematically, in the case where mass transfer occurs predominantly in one direction and where, for simplicity, the mass diffusivity,  $D$ , is taken as constant, we can tackle this limit using the classic one-dimensional diffusion equation,  $C_{,t} = DC_{,yy}$ . As we now show, and as observed in a number of experimental investigations,<sup>[3,4,6]</sup> in the case of titanium casting, the second limit applies.

In order to determine the approximate speed,  $U$ , of the solidification front once it begins to grow away from the mold surface, we employ the energy balance across the phase change interface (and assume for simplicity that no mushy zone exists),  $k_l T_{l,n} - k_s T_{s,n} = \rho U L$ , where the subscripts,  $n$ , denote normal derivatives. (While oxygen contamination leads to formation of a mushy zone, in carrying out an order of magnitude analysis, this effect is expected to be of secondary importance. Specifically, due to a combination of relatively low oxygen concentrations and short solidification times (as subsequently discussed), the presence of a small mushy zone is not expected to significantly alter either the accuracy of the phase interface energy balance given immediately above or the subsequent scaling estimates derived from this balance.) Due to small casting sizes and the large temperature gradients extant, at least during solidification, the liquid and solid-phase heat fluxes into and out of the phase change interface are each of the same order of magnitude as the latent heat release term; thus, we have the approximate relationship  $\rho U L \approx k_s \Delta T / R$ , where again the characteristic temperature difference can be taken as the difference between the initial temperatures of the liquid metal and mold,  $T_0$  and  $T_{mo}$ , respectively. Using the parameter values in Table I, we find that  $U \approx 2(10)^{-3}$  m/s; equally important, the corresponding total solidification time,  $\tau_s \approx R/U$ , is only on the order of 5 seconds.

An estimate of the solid-phase contaminant boundary layer growth rate is readily obtained by balancing the local time rate of the change term in the solid-phase mass-diffusion equation against the dominant radial diffusion term, yielding  $\delta_m \approx \sqrt{D_s t}$ , where  $D_s$  is a characteristic mass diffusivity of oxygen in  $\beta$  titanium. We use the diffusivity of oxygen because atomic oxygen typically comprises the most significant mold constituent in surface alpha layers.<sup>[4,6]</sup> Forming the ratio of  $\delta_m(t)$  to the time-dependent solidification depth,  $\delta_s(t) \approx Ut$ , we finally obtain  $\delta_m / \delta_s \approx 1.4(10^{-3}) / t^{1/2}$ ; thus, for  $t \gg 10^{-6}$  seconds, *i.e.*, for essentially the entire solidification time interval, the melt interface grows much faster and is much thicker than the mass-transfer boundary layer.

The preceding scaling analyses allow us to interpret several well-known experimental observations. (1) The short induction period,  $\tau_I$ , which is proportional to the square of some critical surface asperity length scale,  $\epsilon_a$ , corresponds to a period of high contaminant transport into the casting. As noted by Saha,<sup>[3]</sup> turbulent transport within the bulk liquid metal leads to a subsequent

**Table I. Parameter Values**

Parameter	Magnitude	Reference
$L$	$3.88 \times 10^5 \text{ J kg}^{-1}$	9
$R$	$1.0 \times 10^{-2} \text{ m}$	10
$k_l, k_s$	$2.19 \times 10 \text{ W m}^{-1} \text{ }^\circ\text{C}^{-1}$	11
$T_o$	$2.5 \times 10^3 \text{ }^\circ\text{C}$	12
$T_m$	$1.668 \times 10^3 \text{ }^\circ\text{C}$	11
$T_{mo}$	$8.00 \times 10^2 \text{ }^\circ\text{C}$	3
$\alpha$	$9.22 \times 10^{-6} \text{ m}^2 \text{ s}^{-1}$	11
$\rho$	$4.54 \times 10^3 \text{ N s m}^{-2}$	11
$D_s$	$7.98 \times 10^{-12} \text{ m}^2 \text{ s}^{-1}$	6

uniform bulk distribution of contaminants. (2) The short cast solidification time, which, for the conditions described in References 3, 6, and 7 is only on the order of 5 to 10 seconds, suggests that the liquid-phase contaminant distribution, determined by the rapid mass transfer that occurs during the induction period, becomes frozen into the solidified casting. The magnitude of the bulk contaminant concentration is almost certainly determined by a combination of the length of the induction period,  $\tau_i$ , as well as by the chemical makeup of the mold.<sup>[3,6,7]</sup> (3) Once solidification is complete, due to low solid-phase mass diffusivities, this frozen-in distribution only changes in the thin mass-transfer boundary layer,  $\delta_m$ , located near the mold surface. Importantly, this layer (a) corresponds to the alpha case and (b) grows roughly as  $\sqrt{D_s t}$ . (4) The latter scaling result, indicating that  $\delta_m(t)$  is independent of the concentration of contaminants at the mold surface, is fully consistent with a number of experimental near-surface microhardness measurements;<sup>[1,3,4]</sup> specifically, these studies showed that the depth over which microhardness exhibited significant variation, corresponding to the spatially varying portion of the contaminant distribution, is independent of the mold surface contaminant concentration.

Having determined the essential qualitative nature of the thermophysical processes underlying formation of the alpha case, we can now formulate an appropriate model of the process. In particular, we focus on developing a model of how the contaminant boundary layer grows from the instant that the solidification front grows off of the mold surface, denoting this instant as  $t = 0$ , to the instant,  $t = \tau_0$ , when the casting is removed from the mold. (Note,  $\tau_0$  is on the order of 1 to 3 hours, or, equivalently,  $\tau_0 = O(10^3 \text{ s})$ ).

As an important preliminary, we first introduce an assumption concerning the relationship between casting microhardness and contaminant concentration within the solid phase. Specifically, because oxygen appears to represent the dominant mold constituent taken up in titanium castings,<sup>[4]</sup> we make use of a correlation developed by Saha *et al.*<sup>[6]</sup> relating cast Ti oxygen concentration to microhardness. In developing the correlation, Saha *et al.* carried out Vickers hardness tests (using 50-g loads) on polished 40-mm-diameter Ti buttons, each having a fixed oxygen concentration ranging up to 20,000 ppm (and average grain sizes on the order of 400  $\mu\text{m}$ ).<sup>[6]</sup> The resulting correlation has the form

$$H/H_o = (C/C_o)^m \quad [1]$$

where  $H$  is microhardness,  $C$  is oxygen concentration, and  $H_o$  and  $C_o$  are arbitrarily chosen reference values of microhardness and concentration, respectively. Using Saha's data,<sup>[6]</sup> we take  $H_o = 107 \text{ VHN}$  and  $C_o = 794 \text{ ppm}$ , corresponding to the smallest hardness and associated concentration values reported. In addition, based on Saha's data,<sup>[6]</sup>  $m = 0.56059$ .

Based on the preceding scaling analysis, it is clear that over the time span  $0 \leq t \leq \tau_0$ , contaminant transport near the mold boundary takes place strictly within the

solidified metal and is thus governed by the solid-phase diffusion equation noted earlier. In addition, considering the experiments reported by Saha *et al.*,<sup>[3]</sup> where castings were cylinders having diameters and lengths of  $2(10^{-2}) \text{ m}$  and  $10(10^{-2}) \text{ m}$ , respectively, we assume that transport is strongly one-dimensional, in the inward radial direction. Defining  $y$  as the normal coordinate, directed radially inward from the casting surface,  $y = R - r$ , where  $r$  is the radial coordinate, it is readily shown that because oxygen mass transfer is confined to values of  $y$  much smaller than the cylinder radius,  $R$ , the equation governing oxygen transport into the solidified titanium simplifies to  $C_{,t} = (D_s C_{,y})_{,y}$ . Finally, for simplicity and due to an apparent lack of data concerning the diffusivity of oxygen for temperatures greater than 1425 K,<sup>[6]</sup> we take  $D_s$  as constant.

In order to proceed, we define the solid-phase oxygen concentration relative to the fixed, bulk concentration,  $C_\infty$ , as  $c(y,t) = C(y,t) - C_\infty$ ; it is readily seen that  $c(y,t)$  obeys the same diffusion equation as  $C$ . The boundary conditions and initial condition on  $c$  are as follows. At the mold wall, we assume an effective, constant concentration,  $C_o$ , of soluble oxygen; thus,  $c(y=0, t) = c_o = C_o - C_\infty$ . For large  $y$ , we assume that oxygen transport becomes negligible; thus,  $c_{,y} \rightarrow 0$  as  $y \rightarrow \infty$ . Finally, based on our preceding scaling analysis, we assume that the initial solid-phase concentration is equal to the bulk at the end of the solidification period; thus,  $C(y, t=0) = C_\infty$ , so that  $c(y, t=0) = 0$ . (Note that, in principle,  $C_o$  could be related to the bulk moisture content within a given mold. In order to develop such a relationship, mold porosity, permeability, thermal conductivity, and specific heat, along with the mold's thermal history, would likely be required.)

The solution for the relative concentration field is readily obtained and is given by

$$c(y,t) = c_o \operatorname{erfc} \left( \frac{y}{2\sqrt{D_s t}} \right) \quad [2]$$

where  $\operatorname{erfc}(x)$  is the complimentary error function.

Next, we observe that the near-surface oxygen concentration, as indicated again by near-surface measurements of microhardness, exhibits self-similar structure. This is shown in Figure 1, where we plot microhardness measurements from Saha *et al.*<sup>[3]</sup> in the form of a *relative microhardness function*,  $\psi$ , where the experimental form,  $\psi^{(\text{exp})}$ , is defined as

$$\psi^{(\text{exp})}(y) = \frac{H_{\text{ref}}^n - H_n}{H_{\text{ref}}^n - H_\delta^n} \quad [3]$$

Here,  $H_{\text{ref}} = H(y = y_{\text{ref}}, \tau_0)$ , is the measured microhardness at some arbitrarily defined reference position,  $y = y_{\text{ref}}$ ;  $H = H(y, \tau_0)$  is the position-dependent microhardness;  $H_\delta = H(y = \delta_m, \tau_0)$  is the microhardness at the *nominal* location,  $y = \delta_m$ , where the microhardness profile ceases to exhibit significant spatial variation;  $\tau_0$  is again the total time during which the casting remains in contact with the mold, *i.e.*, the total in-mold cast cooling time; and  $n = 1/m$  is the reciprocal

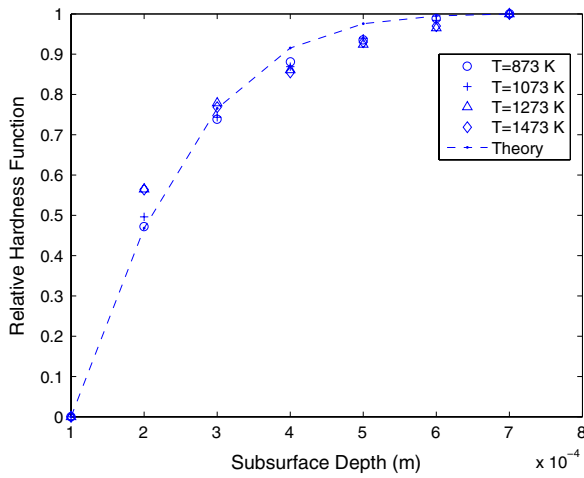


Fig. 1—Comparison of theoretical and experimentally observed subsurface microhardness profiles.

of the exponent  $m$  in Eq. [1]. Based on the measurements reported in Eq. [3], we choose  $y_{\text{ref}} = 100 \mu\text{m}$  and  $\delta_m = 700 \mu\text{m}$ . In addition, we note that  $\tau_0$  is not reported and is thus unknown.

In order to compare the model developed previously with the data in Figure 1, we use the empirical relation [1] in Eq. [3] and obtain

$$\psi^{(\text{theory})}(y) = \frac{\text{erfc}(\chi_{\text{ref}}) - \text{erfc}(\chi)}{\text{erfc}(\chi_{\text{ref}}) - \text{erfc}(\chi_{\delta})} \quad [4]$$

where  $\chi_{\text{ref}} = y_{\text{ref}}/2\sqrt{D_s\tau_0}$ ,  $\chi = y/2\sqrt{D_s\tau_0}$ , and  $\chi_{\delta} = \delta_m/2\sqrt{D_s\tau_0}$ . Note, we do not impose the assumption that the relative concentration at the nominal edge of the mass-transfer boundary layer,  $y = \delta_m$ , is equal to 0.

An unknown parameter,  $D_s\tau_0$ , which is the product of the diffusion coefficient,  $D_s$ , and the in-mold cooling time,  $\tau_0$ , appears in the theoretical expression for  $\psi$  in Eq. [4]. In order to estimate  $D_s\tau_0$ , we assume that  $D_s$  and  $\tau_0$  are both fixed for the sets of experiments described in Eq. [3], and minimize the least-squares fit,

$F = \sum_{j=1}^N [\psi_j^{(\text{exp})} - \psi_j^{(\text{theory})}]^2$ , between the theoretical expression for  $\psi$ , given in Eq. [4], and the experimentally derived expression for  $\psi$  in Eq. [3]. This yields the estimate  $D_s\tau_0 = 2.16(10^{-8})\text{m}^2$ ; using this value in Eq. [4] then yields the theoretical curve shown in Figure 1. Note, if we make the reasonable assumption that  $\tau_0 = O(10^3 \text{ s})$ , then  $D_s = O(10^{-11} \text{ m}^2/\text{s})$ , which is on the order of the diffusion coefficient at the transition temperature ( $T = 1155 \text{ K}$ ) between  $\alpha$  and  $\beta$  titanium.

In summary, scaling analyses have been used to determine the thermal and mass transport processes underlying formation of the alpha case in small titanium castings. Based on this analysis, a simple theoretical model has been developed and used to analyze a typical set of experimental near-surface microhardness measurements.<sup>[3]</sup>

## REFERENCES

1. C. Frueh, D.R. Poirier, and M.C. Maguire: *Metall. Mater. Trans. B*, 1997, vol. 28B, pp. 919–26.
2. S.R. Lyon, S. Inouye, C.A. Alexander, and D.E. Niesz: in *Titanium Science and Technology*, R.I. Jaffe and H.M. Burte, eds., Plenum Press, New York, NY, 1973, vol. 1, pp. 271–84.
3. R.L. Saha, T.K. Nandy, R.D.K. Misra, and K.T. Jacob: *AFS Trans.*, 1990, vol. 98, pp. 253–60.
4. R.L. Saha, T.K. Nandy, R.D.K. Misra, and K.T. Jacob: *Metall. Trans. B*, 1990, vol. 21B, pp. 559–66.
5. V.P. Carey: *Vapor-Liquid Phase Change Phenomena: An Introduction to the Thermophysics of Vaporization and Condensation Processes in Heat Transfer Equipment*, Hemisphere Publishing, New York, NY, 1992, pp. 242–45.
6. R.L. Saha, T.K. Nandy, R.D.K. Misra, and K.T. Jacob: *Bull. Mater. Sci.*, 1989, vol. 12, pp. 481–93.
7. D. Mukherji, R.L. Saha, and C.R. Chakravorty: *Trans. Indian Inst. Met.*, 1985, vol. 38, pp. 465–71.
8. N.R. Harlan, R. Reyes, D.C. Bourell, and J.J. Beaman: *J. Mater. Eng. Performance*, 2001, vol. 4, pp. 410–13.
9. *ASM Handbook, vol. 2, Properties and Selection: Nonferrous Alloys and Special-Purpose Materials*, ASM INTERNATIONAL, Materials Park, OH, 1990.
10. K. Watanabe: Niigata University, Niigata, Japan, private communication, 2001.
11. F.P. Incropera and D.P. DeWitt: *Fundamentals of Heat and Mass Transfer*, Wiley, New York, NY, 1996, p. 830.
12. *Physics of Welding*, J.F. Lancaster, ed., Pergamon Press, New York, NY, 1984.